Dyes and Pigments 89 (2011) 105–110

Contents lists available at ScienceDirect

Dyes and Pigments

journal homepage: www.elsevier.com/locate/dyepig

# Design, synthesis, photoluminescence and electrochemiluminescence properties of naphthalimide derivative and its silver complex

Guiju Hu [a], Liangfei Lv [a], Lin Li [a], Qiong Zhang [a], Xianlei Li [a], Yupeng Tian [a,b,c,*], Jieying Wu [a], Baokang Jin [a,*], Hongping Zhou [a], Jiaxiang Yang [a], Shengyi Zhang [a]

[a] Department of Chemistry, Anhui University and Key Laboratory of Functional Inorganic Materials Chemistry of Anhui Province, Hefei 230039, PR China
[b] State Key Laboratory of Crystal Materials, Shandong University, Jinan 250100, PR China
[c] State Key Laboratory of Coordination Chemistry, Nanjing University, Nanjing 210093, PR China

ARTICLE INFO

*Article history:*
Received 29 May 2010
Received in revised form
1 September 2010
Accepted 3 September 2010
Available online 23 October 2010

*Keywords:*
Naphthalene bisimide (NBI)
Silver complex
Fluorescence
PICT
CV
ECL

ABSTRACT

A new D-A (Donor-Accept) type *N*-(1,2,4-triazolyl)-*N′*-(2-ethylhexyl) naphthalenediimide (**L**) was synthesized. $AgL_2PF_6$ (**1**) and $AgL_2NO_3$ (**2**) were obtained through the reactions of **L** with $AgPF_6$ and $AgNO_3$, respectively. All the compounds were fully characterized. Optical, electrochemical properties and electrogenerated chemiluminescence (ECL) were systematically investigated. Those dual fluorescent emissions for **L**, short wavelength (SW) and long wavelength (LW) emission bands, are rationally explained by the planar intramolecular charge transfer (PICT) model. All the compounds display anodically shift reduction waves with positive reduction potential, compared to its parent compound, Naphthalene bisimide (NBI). It is very interesting that the ECL intensity of the complexes is successfully increased, which is 20 times larger than that of **L**, explaining that the radical anions of the complexes are stabilized by coordinating **L** with Ag(I) ion. The results provide a new approach to study ECL materials.


## 1. Introduction

Electrochemiluminescence (also called electrogenerated chemiluminescence and abbreviated ECL) involves the generation of species at electrode surfaces that then undergo electron-transfer reactions to form excited states that emit light [1]. It has been paid considerable attention over the past several decades due to the inherent essences such as low background signal, simple optical setup, versatility, high sensitivity, and selectivity [2]. The ECL efficiency of luminophores is one of the most important criteria for evaluating the performance of light-emitting materials [3–5]. Most ECL studies for D-A compounds have been developed to tune their photophysical properties through intramolecular charge transfer [6,7] or only to characterize the ECL properties of them [8]. However, in recent years, metal-ligand complexes have played significant important roles in luminescence spectroscopy because of their wide range of absorption and emission wavelengths [9].

Naphthalene bisimide (NBI) derivatives with promising optoelectronic properties have attracted much attention for their potential applications in many areas, such as molecular sensors [10], light harvesting pigments [11], organic semiconductors [12,13], photomolecular switches [14]. Of particular interesting is that as the best n-type molecular semiconductors. This new material reported by Yan et al is a donor-acceptor co-polymer [15], which is highly soluble in common organic solvents and provides the necessary stabilization of the LUMO level. Naphthalene bisimide and its derivatives have also been studied extensively by Wasielewski et al. [16] and other groups [17–21], as an electron acceptor in molecular arrays for photoinduced electron transfer owing to its low reduction potential, its high-lying excited-state and the intense and well-defined spectroscopic signature of the radical anion [22–24]. However, it has been rarely reported up to now that the metal-organic compound or coordination complex based on Naphthalene bisimide has been studied for ECL materials, according to our knowledge, which can merge the merits of organic and inorganic units.

Spurred by those we designed a new D-A type ligand combining Naphthalene bisimide with triazole: *N*-(2-ethylhexyl) *N*-(1,2,4-triazophos) naphthalenediimide (**L**). **L** with the long alkyl chains is highly soluble in common organic solvents, and triazole unit can

* Corresponding authors. Department of Chemistry, Anhui University and Key Laboratory of Functional Inorganic Materials Chemistry of Anhui Province, Hefei 230039, PR China. Tel.: +86 551 5108151; fax: +86 551 5107342.
*E-mail addresses:* yptian@ahu.edu.cn (Y. Tian), bkjinhf@yahoo.com.cn (B. Jin).

0143-7208/$ – see front matter © 2010 Elsevier Ltd. All rights reserved.
doi:10.1016/j.dyepig.2010.09.011

coordinate to metal ions to form metal-organic compounds. At present work, two complexes were obtained by reaction of **L** ligand with Ag-(I) salts. Further more, the electrochemical properties of the **L**, **1** and **2** were systemically investigated. And it is very interesting that the ECL intensities of the complexes are successfully strengthened by coordinating **L** with Ag-(I) ion, which is 20 times larger than that of **L**.

## 2. Experiments

### 2.1. Materials and apparatus

All chemicals and solvents were dried and purified by usual methods. Elemental analysis was performed with a Perkin-Elmer 240B analyzer. IR spectra (4000–400 $cm^{-1}$), as KBr pellets, were recorded on a Nicolet FT-IR 870 SX spectrophotometer. Mass spectra were obtained on a Micromass GCT-MS Spectrometer, and ESI-MS spectra were obtain on a Finnigan LCQ Spectrometer. $^1H$ NMR and $^{13}C$ NMR spectra were recorded on a Bruker AV400 spectrometer with TMS as internal standard.

### 2.2. Optical measurements

UV spectra were recorded on a SHIMADZU UV-3600 spectrophotometer. The fluorescence spectra measurement was performed with use of a HITACHI F-2500 Spectro-fluorophotome. The concentration of sample solution was $1.0 \times 10^{-5}$ mol $L^{-1}$. The fluorescence lifetime was recorded on a Pico Quant floutime 200.

### 2.3. Electrochemistry

Electrochemistry was performed with an MPI-A Electrochemical workstation (Xi An, China). All experiments employed a standard three-electrode cell; the reference electrode was a Ag/AgCl electrode, the auxiliary electrode a platinum wire, and the working electrode a platinum carbon (Pt-C) with a diameter of 1 mm (CV in DMF) (ECL experiments in DMF). The supporting electrolyte was 0.1 M tetrabutylammonium perchlorate (TBAP), in DMF.

### 2.4. Synthesis

#### 2.4.1. Synthesis of N-(2-ethylhexyl) naphthalene monoimide monoanhydride (***L*₀**)

Naphthalene dianhydride (2.00 g, 7.46 mmol) was added into a three-necked flask with 20 ml of freshly distilled DMF. The slurry was heated to about 140 °C under $N_2$ atmosphere, and a little zinc acetate was added into. To this solution, 2-ethylhexylamine (0.97 g, 7.46 mmol) was added drop wise for about 10 min and the reaction mixture was refluxed overnight, under $N_2$ atmosphere. The reaction mixture was cooled, the precipitation appeared was filtered off. DMF was evaporated under low pressure and the insoluble residue was removed by washing with dichloromethane. The dichloromethane solution was evaporated and the crude product was obtained and purified by flash column chromatography (silica, 8:1 petroleum ether: ethyl acetate) to obtain of the desired product $\mathbf{L}_0$ as a pale yellow-orange solid. Yield 25%. IR (KBr, $cm^{-1}$): 3084, 2955, 2928, 2860, 1795, 1759, 1705, 1669, 1582, 1450, 1333, 1285, 1238, 1028, 764, 708; $^1H$ NMR (400 MHz, $CDCl_3$) ppm $\delta = 8.840$ (s, 4H), 4.143–4.207 (m, 2H), 1.917–1.993 (m, 1H), 1.277–1.403 (m, 8H), 0.944–0.981 (t, 3H, $J = 7.4$ Hz), 0.886–0.922 (t, 3H, $J = 7.2$ Hz); MS (EI): *m*/*z*, 379.14.

#### 2.4.2. Synthesis of N-(1,2,4-triazo)-N′-(2-ethylhexyl) naphthalenediimide (***L***)

Compound $\mathbf{L}_0$ (2.83 g, 7.46 mmol) and 4-amino-1,2,4-triazo (1.88 g, 22.39 mmol) were dissolved in a three-necked flask with 20 ml of DMF and refluxed overnight under nitrogen. Subsequently, DMF was evaporated under reduced pressure and the residue was purified by flash column chromatography (silica, 1:1 petroleum ether: ethyl acetate) to get deep-yellow solid of **L**. Yield 70%. IR (KBr, $cm^{-1}$): 3126, 3076, 2960, 2930, 2859, 1737, 1703, 1660, 1581, 1450, 1339, 1244, 1180, 874, 764, 727; $^1H$ NMR (400 MHz, $CDCl_3$): $\delta = 8.867$–$8.917$ (d, 4 H, $J = 7.6$ Hz), 8.415 (s, 2 H), 4.169–4.208 (m, 2 H), 1.903–2.051 (m, 1 H), 1.331–1.452 (m, 8 H), 0.955–0.992 (t, 3 H, $J = 7.4$ Hz), 0.892–0.927 (t, 3 H, $J = 7.0$ Hz) ppm. $^{13}C$ NMR (100 MHz, $CDCl_3$): $\delta = 163.32$, 160.99, 143.54, 131.93, 131.09, 127.89, 126.07, 44.306, 37.685, 30.559, 28.542, 24.007, 22.883, 14.375, 10.881 ppm. MS (EI): *m*/*z*, 445.18.

#### 2.4.3. Synthesis of $AgL_2PF_6$

**L** (0.089 g, 0.2 mmol) was dissolved in dry methanol solution in flask (50 ml), and silver (I) hexafluorophosphate ($AgPF_6$, 0.0250 g, 0.1 mmol) methanol solution was slowly dropped into it. The reaction mixture was refluxed 1 h, cooled and the precipitated complexes were filtered off. The product was transferred immediately to a vacuum desiccator, and dried, 0.015 g product was obtained. IR (KBr, $cm^{-1}$): 3142, 2959, 2929, 2859, 1742, 1712, 1669, 1452, 1339, 1245, 1184, 844, 763, 682, 672, 654; Anal. Calcd. for $C_{48}H_{46}AgF_6N_{10}O_8P$: C, 50.42; H, 4.03; N, 12.26; Found C, 50.21; H, 4.01; N, 12.21; MS-ESI: *m*/*z*, 997.28. $^1H$ NMR (400 MHz, $CDCl_3$): $\delta = 8.888$ (s, 2 H), 8.752–8.815 (d, 4 H, $J = 7.6$ Hz), 4.007–4.056 (m, 2 H), 1.871–1.901 (m, 1 H), 1.268–1.334 (m, 8 H), 0.878–0.915 (t, 3 H, $J = 7.2$ Hz), 0.832–0.865 (t, 3 H, $J = 6.8$ Hz) ppm. $^{13}C$ NMR (100 MHz, [$d_6$]-DMSO): $\delta = 163.33$, 160.97, 143.94, 131.97, 131.09, 127.97, 126.00, 44.307, 37.676, 30.547, 28.541, 23.999, 22.884, 14.388, 10.886 ppm.

#### 2.4.4. Synthesis of $AgL_2NO_3$

**L** (0.089 g, 0.2 mmol) was dissolved in dry methanol solution in flask (50 ml), and silver(I) nitrate ($AgNO_3$, 0.0170 g, 0.1 mmol) acetonitrile solution was slowly dropped into it. The reaction mixture was refluxed 1 h, cooled and the precipitated complexes were filtered off. The product was transferred immediately to a vacuum desiccator and dried, 0.01 g product was obtained. IR (KBr, $cm^{-1}$): 3126, 2960, 2930, 2860, 1741, 1706, 1665, 1583, 1383, 1338, 1244, 1183, 762; Anal. Calcd. for $C_{48}H_{46}AgN_{11}O_{11}$: C, 54.35; H, 4.37; N, 14.52; Found C, 54.13; H, 4.35; N, 14.46; MS-ESI: *m*/*z*, 997.25. $^1H$ NMR (400 MHz, $CDCl_3$): $\delta = 9.006$ (s, 2 H), 8.754–8.823 (d, 4 H, $J = 7.6$ Hz), 4.005–4.053 (m, 2 H), 1.872–1.901 (m, 1 H), 1.269–1.411 (m, 8 H), 0.878–0.915 (t, 3 H, $J = 7.2$ Hz), 0.832–0.865 (t, 3 H, $J = 6.8$ Hz) ppm. $^{13}C$ NMR (100 MHz, [$d_6$]-DMSO): $\delta = 163.31$, 160.92, 144.45, 132.03, 131.10, 128.02, 125.93, 44.313, 37.681, 30.552, 28.543, 23.999, 22.891, 14.391, 10.882 ppm.

## 3. Result and discussion

### 3.1. Preparation of the ligand and its silver complexes

The synthesis of the ligand was illustrated in Scheme 1. The starting material, a precursor of 4-amino-1,2,4-triazole, was prepared in a similar way to the literature method [25] and $\mathbf{L}_0$, a precursor of N-(2-ethylhexyl) naphthalene monoimide monoanhydride, was prepared by an amidation reaction of 2-ethylhexyl in DMF at 140 °C and purified either using recrystallization or column chromatography. The concentration of naphthalene dianhydride to contrast to 2-ethylhexylamine should be less than 1, otherwise the yield of the product will be decreased. We found that

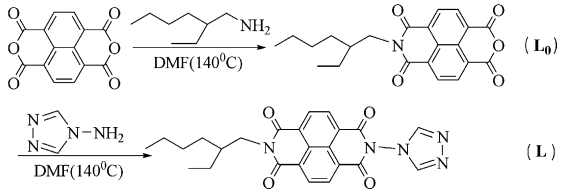


**Scheme 1.** Synthesis of the ligand.

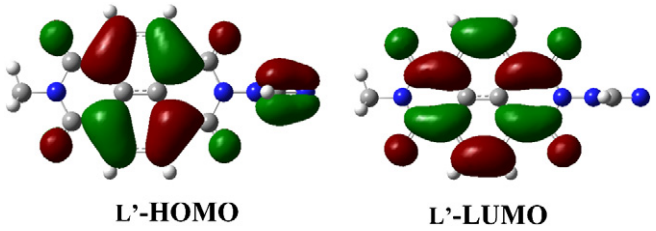


**Fig. 1.** DFT computed frontier orbitals of **L**′ obtained at the B3LYP level.

catalyst, solvent and temperature were also very important to the yield of $\mathbf{L_0}$, and the results were illustrated in Table 1. The structure of ligand **L** was confirmed by IR, $^1$H NMR, and $^{13}$C NMR spectra. The infrared spectrum shows that $\nu_{-C=N-}$ band at 1339 and 1308 cm$^{-1}$ for the triazole group.

The compositions of the complexes of $AgL_2PF_6$ and $AgL_2NO_3$ were confirmed by IR, $^1$H NMR, and $^{13}$C NMR spectra. ESI-Mass spectrometry and elemental analyses were used to further verify the composition of the complexes. The infrared spectra exhibit the characteristic peak of hexafluorophosphate at 884 cm$^{-1}$, and the peak of triazole group red shifted to 1383–1339 cm$^{-1}$. Only the chemical shifts of $\delta_{-N=CH-}$ in the spectra of **1** and **2** changed apparently to the lower field in contrast to the $^1$H NMR spectra of **L**, due to N atom of the triazole group coordinating to and Ag ($\delta = 8.888$, 9.006 ppm, respectively). The $^{13}$C NMR spectra of the complexes (**1** and **2**) show the same trend. The ESI-MS spectra of the complex cations are shown in supporting information Figs. 1 and 2. The measured values ($M^+ = 997.28$, 997.25) agreed well with the calculated ones. Only one strong peak in the figure indicated that the complex cations are very stable in solution. The composition of the complexes has been confirmed from the results above.

### 3.2. Luminescence properties

#### 3.2.1. Computational studies

TDDFT computational studies were perform to elucidate the electronic structures of the ground state of **L**. For this purpose, the model compound **L**′ was used instead of **L**, in which the 2-ethylhexyl group is replaced by a methyl group. Optimizations were carried out with B3LYP [6-31G(d)] without any symmetry restraints, and the TDDFT {B3LYP [6-31G(d)]} calculations were performed on the optimized structure [26]. All calculations, including optimizations and TDDFT, were performed with the G03 software [27]. The optimized structure shows that the NBI (1,4,5,8-naphthalenetetracarboxylic acid bisimide) unit(A) is perpendicular to triazole unit (D) with a dihedral angle of 90°. The spatial plots of selected TDDFT frontier molecular orbitals of **L**′ are shown in Fig. 1 [28].

#### 3.2.2. Single-photon exited fluorescence (SPEF)

The luminescence spectra of the ligand **L** in different solvents with concentration of $C = 1.0 \times 10^{-6}$ mol L$^{-1}$ were shown in Fig. 2 (**1** and **2** in different organic solvents were shown in supporting information, Figs. 3 and 4), and Table 2.

As shown in Fig. 4 and Table 2, it is clear that the emission peaks show no shift with increasing the solvent polarity. This is due to the excited state's activity, so charge redistribution can not take place between the core and the peripheral groups in a very short period of time. On the basis of the above results, we can ignore the solvent effect on the fluorescence spectra for **L**. Of particular interest, **L** displays resolved short wavelength (SW) and long wavelength (LW) emission bands at about 440 nm and 550 nm in $CH_3CN$, respectively. The ligand **L** typically displays only the LW band in benzene, which occurs only a charge-separated twisted ICT (TICT) state based on the dihedral angle between NBI(electron withdrawing group, A) and trizole (electron-donating group, D) group. To illustrate this phenomenon of double fluorescence emission for **L** in acetonitrile, we introduce the model of planar intramolecular charge transfer (PICT) state (Figs. 3 and 4) [29–32].

As shown in Fig. 4, the energy level diagram indicates that excitation state can be formed directly from the Franck-Condon (FC) state through a conical intersection, corresponding to a nonadiabatic and nearly barrierless reaction route [33–35]. Because of steric hindrance a planar internal charge transfer excited state was prevented in the system, but the D-A twist through the torsion of N-N bond in the FC ground states, as a result of the solvation in acetonitrile. The more planar the molecular structure, the stronger the coupling becomes. While electronic excitation generally planarizes the system and thus increases the charge-delocalization (mesomeric) interactions [29], which undergo torsional motion about D-A bond and this is assigned to LW emission. To further prove the interpretation, the fluorescence lifetime of the ligand **L** (at about 440 nm and 550 nm) in acetonitrile has been measured, and those lifetime were 2.52 and 2.54 ns respectively. The results showed that it is reasonable to assume those have the same singlet-state lifetime and also showed the rationality of this model to explain those double fluorescence.

#### 3.2.3. Electrochemistry and Electrochemiluminescence (ECL)

The CV of **L** in DMF solution is shown in Fig. 5 and related data in Table 3. The **L**, at scan rates (v) about 0.1 V/s, shows chemically

**Table 1**
The influence of catalyst and temperature to the yield of $\mathbf{L_0}$.

| Method | Catalyst | Solvent | Temperature (°C) | $L_0$ (yield) |
|---|---|---|---|---|
| a | Non | Imidazole | 100 | 0% |
| b | Non | HOAc | 120 | 0% |
| c | $Zn(OAc)_2$ | *n*-butyl alcohol | 120 | 10% |
| d | $Zn(OAc)_2$ | DMF | 140 | 25% |

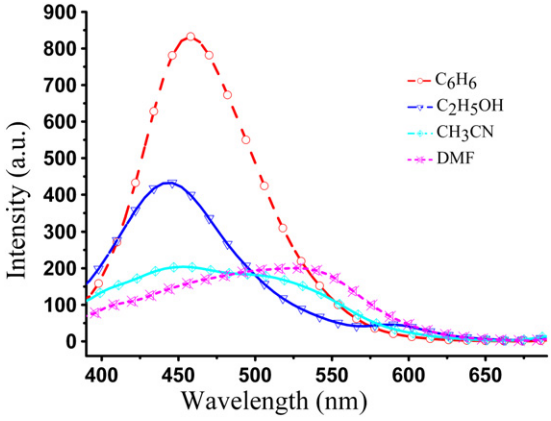


**Fig. 2.** SPEF spectra of **L** in different solvents with $1 \times 10^{-6}$ mol L$^{-1}$.

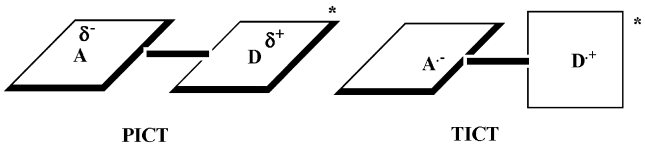


**Fig. 3.** Schematic drawing of geometries and electronic character for the PICT and TICT states of electron donor (D)-acceptor (A) conjugated systems.

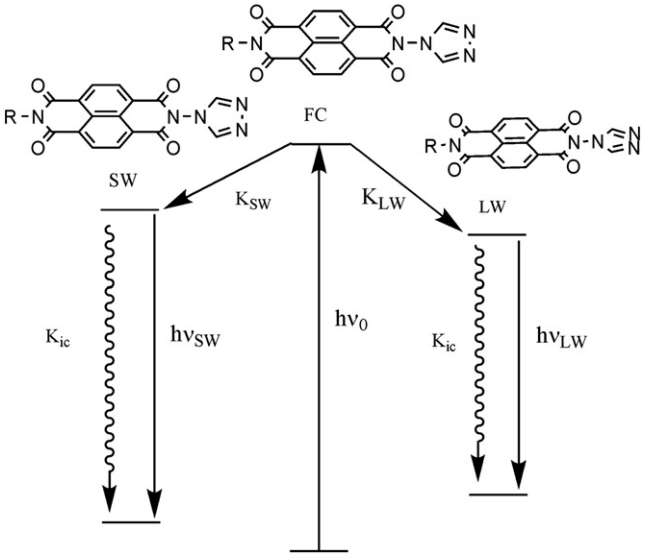


**Fig. 4.** Modified energy level diagram depicting the Franck-Condon state (FC) undergoing vibrational relaxation to SW or LW emission. [a] Structures representing the FC state and the SW state show similar structure whereas the LW state indicates the excited state with extended conjugation (ESEC). (a: As pointed out in Ref. [45], certain components of the SW emission originate from the partial repopulation of SW by the LW excited state. According to the diagram from Wintgens et al., an arrow between these two states is depicted which indicates that these two states are kinetically connected.)

almost reversible waves for the stepwise reduction [two one-electron (1e) transfers] and one 1e oxidation.

The CV of **L** revealed one reversible 1e reduction peak at −0.31 V vs SCE with a second irreversible reduction peak at −0.75 V. The result, compared with that of its parent unit, NBI, reflects strong

**Table 2**
The photophysical data of **L**, **1** and **2** in different solvents.

| Molecules | Solvent | $\varepsilon \times 10^{-4}$ | $\lambda_{max}^{abs}$ | $\lambda_{max}^{SPEF}$ | $\Phi$ |
|---|---|---|---|---|---|
| **L** | Hexane | a, 1.5, 1.6 | a, 364, 382 | a | a |
| | Benzene | 1.3, 1.8, 2.0 | 341, 360, 380 | 457 | 0.12 |
| | Dichloromethane | 1.6, 2.4, 2.7 | 339, 358, 378 | a | 0.54, 0.07 |
| | Ethanol | 0.4, 0.6, 0.7 | 334, 354, 374 | 444, 592 | 0.04, 0.07 |
| | Acetonitrile | 1.5, 2.3, 2.4 | 336, 355, 375 | 453, 502 | 0.13, a |
| | DMF | 1.3, 1.8, 1.9 | 340, 358, 378 | 529 | a |
| **1** | Hexane | 0.2, 0.3, 0.3 | 335, 355, 375 | a | a |
| | Benzene | 2.4, 3.4, 3.7 | 342, 361, 381 | 447 | 0.04 |
| | Dichloromethane | 2.9, 4.5, 5.4 | 342, 359, 379 | a | a |
| | Ethanol | 1.5, 2.4, 2.7 | 338, 357, 376 | 472, 605 | 0.01, 0.01 |
| | Acetonitrile | 2.8, 4.5, 5.3 | 340, 356, 376 | 446, 540 | 0.02, 0.02 |
| | DMF | 2.5, 3.9, 4.5 | 341, 359, 379 | 430 | 0.04 |
| **2** | Hexane | 0.3, 0.4, 0.4 | 335, 355, 375 | a | a |
| | Benzene | 1.6, 2.4, 2.6 | 343, 361, 380 | 468 | 0.05 |
| | Dichloromethane | 2.2, 3.4, 4.1 | 342, 359, 380 | a | a |
| | Ethanol | 1.6, 2.4, 2.7 | 340, 356, 376 | 459, 615 | 0.10, 0.02 |
| | Acetonitrile | 2.1, 3.4, 4.0 | 339, 356, 376 | 442, 540 | 0.05, 0.01 |
| | DMF | 2.0, 3.0, 3.5 | 341, 359, 379 | 441 | 0.05 |

$\varepsilon_{max}$: The corresponding molar absorption coefficient, $\lambda_{max}^{abs}$: $l_{max}$ of the UV absorption spectra in nm, $\lambda_{max}^{SPEF}$: $l_{max}$ of the SPEF spectra in nm. [a] not tested.

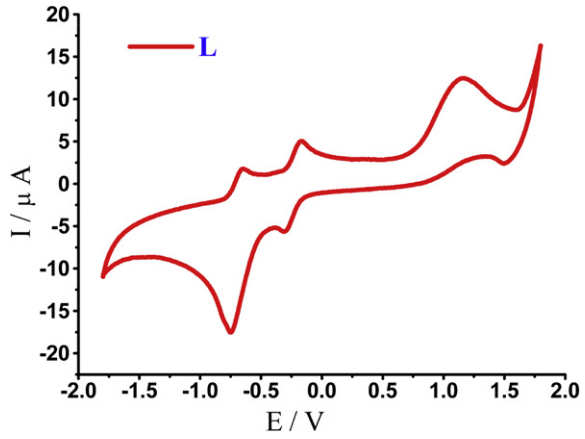


**Fig. 5.** Cyclic Votammogram (0.1 V/s) of **L** ($1 \times 10^{-5}$ mol $L^{-1}$) in DMF with 0.1 M $Bu_4NClO_4$.

**Table 3**
Electrochemical Data of **L**, **1** and **2** recorded in DMF containing 0.1 M of $Bu_4NClO_4$ as supporting electrolyte and referenced versus a saturated calomel electrode (SCE).

| | $E_{Red}$ (V) | | $E_{Ox}$(V) |
|---|---|---|---|
| | $NBI^-/NBI^{2-}$ | $NBI/NBI^-$ | $NBI/NBI^+$ |
| **L** | −0.66 | −0.31 | 1.66 |
| **1** | −0.62 | −0.54 | 0.43 |
| **2** | −0.66 | −0.64 | 0.41 |

electron-accepting nature of the carboximide subsitituent in **L**, and displays anodically shift reduction waves with positive reduction potential. In contrast, the triazole unit in the molecule enhances electronic π-conjugation and induces a stabilization of LUMO frontier molecular orbital, thus rendering the molecule more reducible than the unsubstituted naphthalene bisimide. In ligand **L**, the high lying HOMO along with the stabilized LUMO explains the appearance of a low energy transition observed in the visible absorption spectrum. With such a low reduction potential, this molecule will certainly be useful as a final electron acceptor in molecular arrays for long-range electron transfer or for the development of materials exhibiting *n*-type conducting behavior [22,36].

The proposed reduction mechanism for the diimide systems is shown in Scheme 2 [37], where the 1e transfer processes lead to the formation of a radical anion and then the dianion. It is reasonable to assume that the major portion of electron density resides on the carbonyl oxygen due to the electron-withdrawing nature of the oxygen atom as indicated in possible resonance forms in Scheme 2.

In order to check the influence of the coordinated silver (I) on the reduction potential, the CV of the complexes were recorded in the same condition in Table 3. (The CV curves Figs. 5 and 6 are given in the Supporting Information). The negative shifts are observed for the two reduction peaks in the CV curve of the complexes. The electronic density of the core decreases, due to the electron-withdrawing silver (I) coordinated to the N atom of the triazole group,

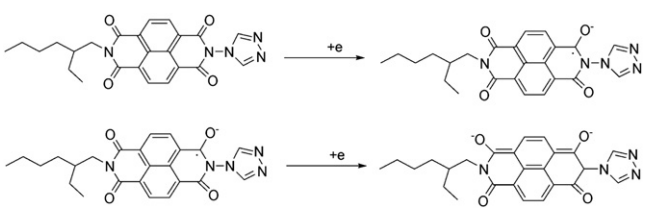


**Scheme 2.** Proposed two-step reduction mechanism for the **L**.

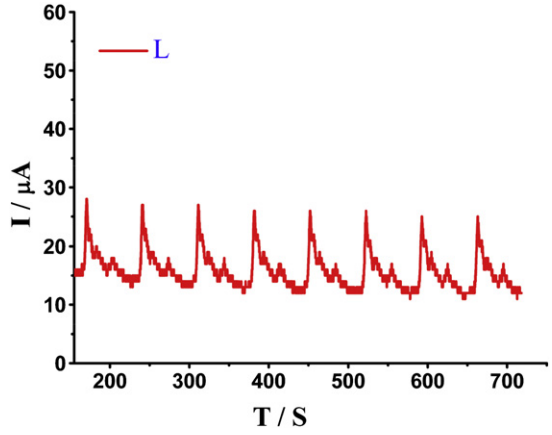


**Fig. 6.** Electrochemiluminescence of **L** ($1 \times 10^{-5}$ mol $L^{-1}$) in DMF with 0.1 M $Bu_4NClO_4$ under continuous cyclic voltammetry with the scan rate of 0.1 V/s.

which made the reduction waves shift to more negative regions through the electron delocalization in the π-conjugation system. The silver's electron-withdrawing function can be further illustrated by the oxidation wave for the two complexes with significantly negative shifts.

For further studying the influence of the silver (I) on electrochemical behavior, a series of ECL emission tests were performed in DMF solution containing **L** or the complexes 1 mM, and the ECL intensity were shown in Figs. 6 and 7, respectively (Electrochemiluminescence of **2** is given in the Supporting Information Fig. 6).

Of particularly interest, we found that the ECL intensity of the complexes exhibit about 20 times larger than that of **L**, shown in Figs. 6 and 7. There was almost no detectable changing for ECL intensities, indicating the stability of the ECL emission of the complexes. According to the Fig. 8 [38], we proposed the mechanism of the three compounds ECL emission in following Scheme 3. That is, to be energy-sufficient to produce singlet state electrochemiluminescence, an oxidation reaction by a species (R) and the first perylene reduction wave is required, so that the following can occur subsequent annihilation reaction between these two ions generates excited states that lead to emission (eqs. 3 and 4).

The reason for the much higher ECL intensity of the complexes, is the good stability of the complexes radical anion ($R^{\bullet}$). When the Pt electrode is pulsed to generate the radical cation and anions stepwisely, the stability of $R^{\bullet}$ will greatly enhanced the ECL

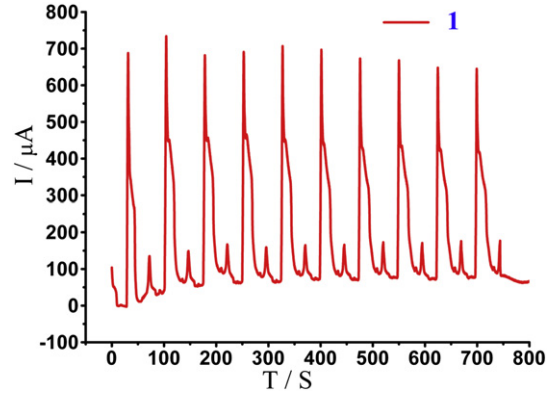


**Fig. 7.** Electrochemiluminescence of **1** ($1 \times 10^{-5}$ mol $L^{-1}$) in DMF with 0.1 M $Bu_4NClO_4$ under continuous cyclic voltammetry with the scan rate of 0.1 V/s.

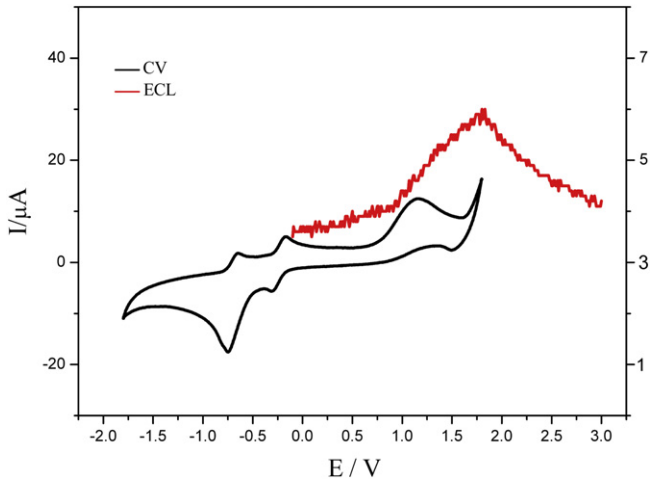


**Fig. 8.** ECL emission spectra obtained from in DMF solution containing the **L** 0.1 M at the scan rate of 0.1 V/s. In order to compare with the CV curve, the ECL intensity of **L** was subtracted 15.

$$R - e \longrightarrow R^{\bullet+} \quad (1)$$

$$R + e \longrightarrow R^{\bullet-} \quad (2)$$

$$R^{\bullet+} + R^{\bullet-} \longrightarrow {}^1R^* + R \quad (3)$$

$${}^1R^* \longrightarrow R + h\nu \quad (4)$$

**Scheme 3.** Proposed ECL emission for the **L**, **1** and **2**.

intensity. Interestingly, the photoluminescence intensity of the complexes is much lower than that of **L** in solution, and those emission bands are almost not changed. But the ECL emission intensities of the complexes were enhanced compared with those of **L**. This may be attributed to the different mechanisms between the photoluminescence and ECL emission, for that metal ion can be good quenchers because of photoninduced energy and charge transfer (CT) [39].

## 4. Conclusion

In this work, a novel D-A ligand **L** and its two silver complexes have been synthesized and fully characterized. The negative shifts were observed for two reduction peaks in the CV curve for the complexes. Particular interest is the low reduction potential of the complexes, and about 20 times of the increased ECL emission intensity compared with those of the ligand **L**. Significantly, the findings provides a new pathway to design and synthesise ECL emission materials.

## Acknowledgments

This work was supported by a grant for the National Natural Science Foundation of China (20771001, 20775001 and 20875001), the Team for Scientific Innovation Foundation of Anhui Province (2006KJ007TD), Department of Education Committee of Anhui Province (KJ2010A030).

## References

[1] Richter MM. Electrochemiluminescence (ECL). Chemical Reviews 2004;104 (6):3003–36.
[2] Du Y, Qi B, Yang XR, Wang EK. Journal of Physical Chemistry B 2006;110 (43):21662–6.

[3] Liu X, Shi L, Niu W, Li H, Xu G. Environmentally friendly and highly sensitive ruthenium(II) tris(2,2′-bipyridyl) electrochemiluminescent system using 2-(dibutylamino)ethanol as co-reactant. Angewandte Chemie 2007;119(3):425–8.
[4] Booker C, Wang X, Haroun S, Zhou J, Jennings M, Pagenkopf BL, et al. Tuning of electrogenerated silole chemiluminescence. Angewandte Chemie 2008;120 (40):7845–9.
[5] Rashidnadimi S, Hung TH, Wong KT, Bard AJ. Electrochemistry and electrogenerated chemiluminescence of 3,6-di(spirobifluorene)-*N*-phenylcarbazole. Journal America Chemistry Society 2008;130(2):634–9.
[6] Marsden JA, Miller JJ, Shirtcliff LD, Haley MM. Structure-property relationships of donor/acceptor-functionalized tetrakis(phenylethynyl)benzenes and bis (dehydrobenzoannuleno)benzenes. Journal America Chemistry Society 2005;127(8):2464–76.
[7] Elangovan A, Kao KM, Yang SW, Chen YL, Ho TI, Su YO. Synthesis, electronic properties, and electrochemiluminescence of donor-substituted phenylethynylanthronitriles. Journal Organic Chemistry 2005;70(11):4460–9.
[8] Oh JW, Lee YO, Kim TH, Ko KC, Lee JY, Kim H, et al. Enhancement of electrogenerated chemiluminescence and radical stability by peripheral multidonors on alkynylpyrene derivatives. Angewandte Chemie International Edition 2008;47(1):1–4.
[9] Gobetto R, Caputo G, Garino C, Ghiani S, Nervi C, Salassa L, et al. Synthesis, electrochemical and electrogenerated chemiluminescence studies of ruthenium (II) bis(2,2′-bipyridyl){2-(4-methylpyridin-2-yl)benzo[d]-X-azole} complexes. European Journal of Inorganic Chemistry 2006;12(14):2839–49.
[10] (a) Rogers E, Kelly LA. Nucleic acid oxidation Mediated by Naphthalene and benzophenone imide and diimide derivatives: consequences for DNA redox chemistry. Journal America Chemistry Society 1999;121(16):3854–61;
(b) Adhikiri, Heagy MD. Fluorescent chemosensor for carbohydrates which shows large change in chelation-enhanced quenching. Tetrahedron Letters 1999;40(45):7893–6;
(c) Hunter CA, Tregonning R. Modular assembly of porphyrin sandwiches as potential hosts. Tetrahedron 2002;58(4):91–697.
[11] Röger C, Muller MG, Lysetska M, Miloslavina Y, Holzwarth AR, Wurthner F. Efficient energy transfer from peripheral chromophores to the self-assembled zinc chlorin rod antenna: a bioinspired light-harvesting system to bridge the "Green Gap". Journal of America Chemistry Society 2006;128(20):6542–3.
[12] Katz HE, Lovinger AJ, Johnson J, Kloc C, Slegrist T, Li W, et al. A soluble and air-stable organic semiconductor with high electron mobility. Nature 2000;404 (30):478–81.
[13] Jones BA, Ahrens MJ, Yoon MH, Facchetti A, Marks TJ, Wasielewski MR. Angewandte Chemie International Edition 2004;43(46):6363–6.
[14] (a) Gosztola D, Niemczyk MP, Wasielewski MR. Picosecond molecular switch based on bidirectional inhibition of photoinduced electron transfer using photogenerated electric fields. Journal of America Chemistry Society 1998;120 (20):5118–9;
(b) Hayes RT, Wasielewski MR, Gosztola D. Ultrafast photoswitched charge transmission through the bridge molecule in a donor-bridge-acceptor system. Journal of America Chemistry Society 2000;122(23):5563–7;
(c) Lukas AS, Bushard PJ, Wasielewski MR. Journal of America Chemistry Society 2001;123(10):2440–1.
[15] Sirringhaus H. Electrons in the fast lane. Nature 2009;457(5):667–8;
(b) Yan H, Chen ZH, Zheng Y, Newman C, Quinn JR, Dötz F, et al. A high-mobility electron-transporting polymer for printed transistor. Nature 2009;457(5):679–86.
[16] (a) Wasielewski MR. Energy, charge, and spin transport in molecules and self-assembled nanostructures inspired by photosynthesis. Journal of Organic Chemistry 2006;71(14):5051–66;
(b) Greenfield SR, Svec WA, Gosztola D, Wasielewski MR. Multistep photochemical charge separation in rod-like molecules based on aromatic imides and diimides. Journal of America Chemistry Society 1996;118(28):6767–77;
(c) Wiederrecht GP, Niemczyk MP, Svec WA, Wasielewski MR. Ultrafast photoinduced electron transfer in a chlorophyll-based triad: vibrationally hot ion pair intermediates and dynamic solvent effects. Journal of America Chemitry Society 1996;118(28):81–8.
[17] (a) Shiratori H, Ohno T, Nozaki K, Yamazaki I, Nishimura Y, Osuka A. Coordination control of intramolecular electron transfer in boronate-bridged zinc porphyrin-diimide molecules. Journal Organic Chemitry 2000;65(25):8747–57;
(b) Osuka A, Yoneshima R, Shiratori H, Osuka A, Okada T, Taniguchi S, et al. Electron transfer in a hydrogen-bonded assembly consisting of porphyrin–diimide. Chemistry Communication; 1998:1567–8.
[18] (a) Mataga N, Chosrowjan H, Shibata Y, Yoshida N, Osuka A, Kikuzawa T, et al. First unequivocal observation of the whole bell-shaped energy gap law in intramolecular charge separation from $S_2$ excited state of directly linked Porphyrin–Imide dyads and its solvent-polarity dependencies. Journal of America Chemistry Society 2001;123(49):12422–3;
(b) Okamoto K, Mori Y, Yamada H, Imahori H, Fukuzumi S. Effects of Metal ions on photoinduced electron transfer in zinc porphyrin-naphthalenediimide linked systems. Chemistry European Journal 2004;10(2):474–83;
(c) Mori Y, Sakaguchi Y, Hayashi H. Spin effects on decay dynamics of charge-separated states generated by photoinduced electron transfer in zinc porphyrin–naphthalenediimide dyads. Journal of Physical Chemistry A 2002;106 (18):4453–67.
[19] (a) Johansson O, Borgström M, Lomoth R, Palmblad M, Bergquist J, Hammarström L, et al. Electron donor-acceptor dyads based on ruthenium(II) bipyridine and terpyridine complexes bound to naphthalenediimide. Inorganic Chemistry 2003;42(9):2908–18;
(b) Abraham B, McMasters S, Mullan MA, Kelly LA. Reactivities of carboxyalkyl-substituted 1,4,5,8-naphthalene diimides in aqueous solution. Journal America Chemistry Society 2004;126(13):4293–300.
[20] Dixon DW, Thornton NB, Steullet V, Netzel T. Effect of DNA scaffolding on intramolecular electron transfer quenching of a photoexcited ruthenium(II) polypyridine naphthalene diimide. Inorganic Chemistry 1999;38(24): 5526–34.
[21] Chaignon F, Falkenström M, Karlsson S, Blart E, Odobel F, Hammarström L. Very large acceleration of the photoinduced electron transfer in a Ru(bpy) 3–naphthalene bisimide dyad bridged on the naphthyl core. Chemistry Communication; 2007:64–6.
[22] Gosztola D, Niemczyk MP, Svec W, Lukas AS, Wasielewski MR. Excited doublet states of electrochemically generated aromatic imide and diimide radical anions. Journal of Physical Chemistry A 2000;104(28):6545–51.
[23] Chopin S, Chaignon F, Blart E, Odobel F. Syntheses and properties of core-substituted naphthalene bisimides with aryl ethynyl or cyano groups. Journal of Material Chemistry 2007;17(39):4139–46.
[24] Le TP, Rogers JE, Kelly LA. Journal Physical Chemistry A 2000;104(29): 6778–85.
[25] (a) Herbst RM, Garrison JA. A study on the formation of 4-amino-triazolederivatives from acyl hydrazides. Journal Organic Chemistry 1953;18 (7):827–77;
(b) Raidt M, Neuburger M, Kaden TA. Stability and structure of mono- and dinuclear Cu(II), Ni(II) and Zn(II) complexes of pyrazole and triazole bridged bis-macrocycles. Dalton Transactions 2003;3(7):1292–8.
[26] Yang L, Feng JK, Ren AM. Theoretical study on electronic structure and optical properties of phenothiazine-containing conjugated oligomers and polymers. Journal of Organic Chemisrty 2005;70(15):5987–96.
[27] Frisch MJ, Trucks GW, Schlegel HB, Scuseria GE, Robb MA, Cheeseman JR, et al. Gaussian 03, Revision B.04. Pittsburgh, PA: Gaussian, Inc.; 2003.
[28] Li DM, Hu RT, Zhou W, Sun PP, Kan YH, Tian YP, et al. Synthesis, structures, and photophysical properties of two organostannoxanes from a novel acrylic acid derived from phenothiazine. European Journal of Inorganic Chemistry; 2009:2664–72.
[29] (a) Sluch MI, Godt A, Bunz UHF, Berg MA. Excited-state dynamics of Oligo(*p*-phenyleneethynylene): quadratic coupling and torsional motions. Journal of America Chemistry Society 2001;123(26):6447–8;
(b) Yang JS, Yan JL, Hwang CY, Chiou SY, Liau KL, Tsai HSG, et al. Probing the intrachain and interchain effects on the fluorescence behavior of pentiptycene-derived Oligo(*p*-phenyleneethynylene)s. Journal of America Chemistry Society 2006;128(43):14109–19.
[30] Rettig W. Charge separation in excited states of decoupled systems TICT compounds and implications regarding the development of processes and the development of new laser dyes and the primary process of vision and photosynthesis. Angewandte Chemie International Edition 1986;25:971–88;
(b) Rettig W, Maus M. Conformational analysis of molecules in excited states. New York: Wiley, VCH; 2000. pp. 1–5.
[31] Cao H, Chang V, Hernandez R, Heagy MD. Matrix screening of substituted *N*-Aryl-1,8-naphthalimides reveals new dual fluorescent dyes and unusually bright pyridine derivatives. Journal of Organic Chemistry 2005;70(13): 4929–34.
[32] Yang JS, Liau KL, Li CY, Chen MY. Meta conjugation effect on the torsional motion of aminostilbenes in the photoinduced intramolecular charge-transfer state. Journal of America Chemistry Society 2007;129(43):13183–92.
[33] Grabowski ZR, Rotkiewicz K. Structural changes accompanying intramolecular electron transfer: focus on twisted intramolecular charge-transfer states and structures. Chemistry Review 2003;103(10):3899–4031.
[34] Fuss W, Pushpa KK, Rettig W, Schmid WE, Trushin SA. Ultrafast charge transfer via a conical intersection in dimethylaminobenzonitrile. Photochemistry Photobiology Society 2002;1:255–62.
[35] Gómez I, Reguero M, Pasqua MB, Robb MA. Journal of America Chemistry Society 2005;127(19):7119–29.
[36] Jones BA, Ahrens MJ, Yoon MH, Facchetti A, Marks TJ, Wasielewski MR. High-mobility air-stable n-type semiconductors with processing versatility: dicyanoperylene-3,4:9,10-bis(dicarboximides). Angewandte Chemie International Edition 2004;43(46):6363–6.
[37] Lee SK, Zu YB, Herrmann A, Geerts Y, Müllen K, Bard AJ. Electrochemistry, spectroscopy and electrogenerated chemiluminescence of perylene, terrylene, and quaterrylene diimides in aprotic solution. Journal of America Chemistry Society 1999;121(14):3513–20.
[38] Zanarini S, Rampazzo E, Bich D, Canteri R, Ciana LD, Marcaccio M, et al. Synthesis and electrochemiluminescence of a $Ru(bpy)_3$-Labeled coupling adduct produced on a self-assembled monolayer. Journal of Physical Chemistry C 2008;112(8):2949–57.
[39] Zheng QD, He GS, Prasad PN. Novel two-photon-absorbing, 1,10-phenanthroline-containing Л-conjugated chromophores and their nickel(II) chelated complexes with quenched emissions. Journal of Materials Chemistry 2005;15:579–87.